Clinical Neurophysiology Practice 5 (2020) 1–9

Contents lists available at ScienceDirect

Clinical Neurophysiology Practice

journal homepage: www.elsevier.com/locate/cnp

Very early Guillain-Barré syndrome: A clinical-electrophysiological and ultrasonographic study

José Berciano [a,*], Pedro Orizaola [b], Elena Gallardo [c], Ana L. Pelayo-Negro [a], Pascual Sánchez-Juan [a], Jon Infante [a], María J. Sedano [a]

[a] Service of Neurology, University Hospital "Marqués de Valdecilla (IDIVAL)", University of Cantabria, "Centro de Investigación Biomédica en Red de Enfermedades Neurodegenerativas (CIBERNED)", Santander, Spain
[b] Service of Clinical Neurophysiology, University Hospital "Marqués de Valdecilla (IDIVAL)", Santander, Spain
[c] Service of Radiology, University Hospital "Marqués de Valdecilla (IDIVAL)", University of Cantabria, "Centro de Investigación Biomédica en Red de Enfermedades Neurodegenerativas (CIBERNED)", Santander, Spain

ARTICLE INFO

Article history:
Received 4 September 2019
Received in revised form 24 October 2019
Accepted 8 November 2019
Available online 30 November 2019

Keywords:
Axonal degeneration
Demyelination
Endoneurial inflammatory oedema
Guillain-Barré syndrome
Ultrasonography
Very early Guillain-Barré syndrome

ABSTRACT

Objectives: Using recent optimized electrodiagnostic criteria sets, we primarily aimed at verifying the accuracy of the initial electrophysiological test in very early Guillain-Barré syndrome (VEGBS), ≤4 days of onset, compared with the results of serial electrophysiology. Our secondary objective was to correlate early electrophysiological results with sonographic nerve changes.
Methods: This is a retrospective study based on consecutive VEGBS patients admitted to the hospital. Each patient had serial nerve conduction studies (NCS) in at least 4 nerves. Initial NCS were done within 4 days after onset, and serial ones from the second week onwards. Electrophysiological recordings of each case were re-evaluated, GBS subtype being established accordingly. Nerve ultrasonography was almost always performed within 2 weeks after onset.
Results: Fifteen adult VEGBS patients were identified with a mean age of 57.8 years. At first NCS, VEGBS sub-typing was only possible in 3 (20%) cases that showed an axonal pattern, the remaining patterns being mixed (combining axonal and demyelinating features) in 6 (40%), equivocal in 5 (33.3%), and normal in 1 (6.7%). Upon serial NCS, 7 (46.7%) cases were categorized as acute demyelinating polyneuropathy, 7 (46.7%) as axonal GBS, and 1 (6.6%) as unclassified syndrome. Antiganglioside reactivity was detected in 5 out of the 7 axonal cases. Nerve US showed that lesions mainly involved the ventral rami of scanned cervical nerves.
Conclusions: Serial electrophysiological evaluation is necessary for accurate VEGBS subtype classification. Ultrasonography helps delineate the topography of nerve changes.
Significance: We provide new VEGBS pathophysiological insights into nerve conduction alterations within the first 4 days of the clinical course.

1. Introduction

Guillain-Barré syndrome (GBS) is an acute-onset, immune mediated disorder of the peripheral nervous system, which includes at least three disease patterns: acute inflammatory demyelinating polyneuropathy (AIDP), acute motor axonal and motor-sensory axonal neuropathy (AMAN and AMSAN) and Miller-Fisher syndrome (MFS) (Griffin et al., 1996; van den Berg et al., 2014). Furthermore, GBS and MFS are sub-classified into classic and localized forms (Wakerley et al., 2014). AMAN/AMSAN and MFS are associated with anti-ganglioside reactivity.

Nerve conduction studies (NCS) play an important role in GBS diagnosis and subtype classification (Hadden et al., 1998; Rajabally et al., 2015; Uncini and Kuwabara, 2018). It is debated whether the GBS subtypes can be diagnosed by a single electrophysiological study; given that GBS pathophysiology is dynamic, serial studies seem to allow a more accurate diagnosis of subtypes (Uncini et al., 2017). The accuracy of electrodiagnostic GBS subtyping has been optimized by adding, to existing criteria sets, duration of motor responses and reversible conduction failure (RCF) in motor and sensory nerves upon serial evaluation (Uncini and Kuwabara, 2018). In early GBS stages, arbitrarily encompassing patients who underwent nerve conduction studies within 7 or

* Corresponding author at: University of Cantabria, Department of Medicine and Psychiatry, EUE Building (4th Floor), Avda. Valdecilla s/n, 39008 Santander, Spain.
E-mail address: jaberciano@humv.es (J. Berciano).

https://doi.org/10.1016/j.cnp.2019.11.003
2467-981X/

10 days after onset, electrophysiology frequently reveals abnormalities that are not specific of primary demyelinating neuropathy (Gordon and Wilbourn, 2001; Vucic et al., 2004; Chanson et al., 2014). Reports focusing on the very early stages of GBS (VEGBS), ≤4 days after onset, indicate that 67% of electrodiagnostic studies are classified as equivocal (Albertí et al., 2011). To the best of our knowledge, there are no previous studies for establishing the diagnostic accuracy of optimized electrophysiology in VEGBS.

Nerve ultrasonography (US) has emerged as promising technique in the diagnosis of peripheral nervous system disorders (Gallardo et al., 2015b). In VEGBS, US may show extensive enlargement of cross-sectional areas (CSA) in all nerves except of ulnar and sural nerves (Grimm et al., 2014, 2016). In early GBS we have reported that main US changes rely on ventral rami of C5-C7 nerves, consisting of significant increase of their CSA and blurred boundaries (Gallardo et al., 2015a). Such imaging findings are in good correlation with autopsy features in early stages of the disease showing that endoneurial inflammatory oedema is the outstanding lesion predominating in proximal nerve trunks (Gallardo et al., 2015a; Berciano et al., 2017).

Using Uncini's optimized electrodiagnostic criteria of GBS subtypes (Uncini et al., 2017), our primary objective was to analyse the diagnostic accuracy at first electrophysiological test in VEGBS patients compared with the results of serial electrophysiological evaluation. Our secondary objective was to correlate early electrophysiological features with topographic US nerve changes.

2. Methods

2.1. Patients

This is a retrospective study based on consecutive GBS patients attended at the University Hospital "Marqués de Valdecilla", between 2011 and 2018, whose initial electrophysiological evaluation was carried out between days 1 and 4 of clinical onset. We included patients with clinical data, laboratory tests and electrophysiological results suggestive of classic GBS (Wakerley et al., 2014; Asbury and Cornblath, 1990), with the exception of one patient showing paraparetic axonal GBS (Berciano et al., 2016). Clinical evaluation was done following the protocol reported in two previous studies (Sedano et al., 1994, 2019). Clinical data recorded during the acute phase of the illness included demography, type of antecedent events and duration of the progressive phase. Neurological manifestations at the nadir comprised motor weakness distribution, involvement of cranial nerve, sensory loss, presence of pain, and need of mechanically ventilated disease. Eight cases of the series have been included in the IGOS study (Doets et al., 2019), and 12 of them in a recent descriptive GBS survey carried out in our Institution (Sedano et al., 2019).

Standardized examination involved evaluation of muscle power according to the Medical Research Council. Patients were graded using GBS disability (GBSd) score, adapted from Winner and colleagues (Winer et al., 1988): 0 = healthy; 1 = minimal symptoms or signs; 2 = able to walk without assistance, but unable to do manual work; 3 = able to walk with assistance; 4 = chair/bed bound; 5 = mechanically ventilated; and 6 = dead. Leaving one deceased patient aside, serial examination was systematically carried out for a period ranging between 8 and 24 months after onset.

This investigation was approved by the Local Ethics Committee.

2.2. Electrophysiological studies

Electromyography and NCS were performed using standard techniques as reported elsewhere (Berciano et al., 2000). For the current study, electrophysiological recordings were blinded re-evaluated by two of us (PO and JB), classification being done according to optimized GBS criteria sets (Uncini et al., 2017) (Supplementary material, Table S1).

At first electrodiagnostic evaluation (days 1–4), NCS were performed in an ipsilateral upper extremity and lower extremity; motor NCS was routinely estimated in median, ulnar, tibial and peroneal nerves, and sensory NCS in median, ulnar, sural and superficial peroneal nerves. Motor conduction parameters analyzed were as follows: motor conduction velocity (MCV), distal motor latency (DML), compound muscle action potential amplitude (CMAP; from baseline to negative peak), CMAP duration (from first negative defection to return to baseline of the last negative deflection), minimal F-wave latency, proximal CMAP (pCMAP)/distal CMAP (dCMAP) amplitude ratio, and pCMAP/dCMAP duration ratio. dCMAP duration and temporal dispersion of median, ulnar, tibial and peroneal nerves were evaluated in accordance with Clouston and colleagues' criteria (Clouston et al., 1994). F-wave latencies were measured with each motor NCS for which a CMAP result was obtained. Sensory conduction parameters included peak-to-peak amplitude of sensory nerve action potential (SNAP) and sensory conduction velocity (SCV). Both in motor and sensory nerves, potential RCF was evaluated on serial electrophysiological studies.

Repeated electrophysiological studies, two or more times, were done at variable intervals, but always from the second week onwards.

2.3. Laboratory investigations

Routine laboratory analyses included cerebrospinal examination and antiganglioside reactivity testing, this not being available in two cases. Serum samples, collected in the first few days of the clinical course, were tested by the line-blot EUROLINE Antiganglioside Profiles (Euroimmun, Medizinische, Labordiagnostika, AG) for IgG/IgM antibodies against GM1, GM2, GM3, GD1a, GD1b and GQ1b.

2.4. Ultrasonographic study

US examination was performed as reported elsewhere (Gallardo et al., 2015a) and within the first two weeks after onset with just one exception. Bilaterally, we studied C5–C7 nerves, median nerve and ulnar nerve (at upper arm and forearm), radial nerve (at antecubital fossa), tibial nerve (at popliteal fossa and ankle), peroneal nerve (at popliteal fossa) and sural nerve (at ankle).

2.5. Statistical analysis

Quantitative variables were described by means and standard deviations and qualitative variables by percentages. Comparisons between quantitative variables were performed with Student's T test. All statistical tests were performed using SPSS software (version 20).

3. Results

3.1. Clinical and laboratory findings

Clinical and laboratory features are summarized in Table 1. The series comprises 15 patients presenting with classic GBS, namely all of them exhibited ascending flaccid and areflexic weakness leading to quadriparesis in 14, or paraparesis in 1. Around half the patients showed sensory loss or nerve trunk pain, and a quarter of total exhibited cranial nerve involvement. Ages at diagnosis ranged between 18 and 80 years (mean 57.8). The male/female ratio

Table 1
Clinical features.

Case No	Age	Sex	Prodromic event weeks	Interval onset-nadir score	Peak GBSd	GBSd at 1 yr	GBSd at 2 yrs	Antiganglioside antibodies	Final diagnosis
1	64	M	Diarrhoea	1	4	3	2	GM1, GD1a	AMSAN
2	59	F	Diarrhoea	2	5	2	2	Negative	AIDP
3	69	M	Diarrhoea	1	5	5	4[a]	GM1	AMSAN
4	24	F	No	2	2	1	1	Not studied	AIDP
5	80	F	Diarrhoea	1	5	NA[b]	NA	GM1, GD1a	AMSAN
6	18	F	Diarrhoea	1	4	2	1	Negative	Axonal GBS[c]
7	77	M	URTI	1	5	0	0	Negative	AIDP
8	43	M	Diarrhoea	1	4	3	2	GM1	AMAN
9	42	F	URTI	1	2	0	0	Negative	AIDP
10	62	M	Diarrhoea	1	2	2	2	Negative	Unclassified
11	74	M	URTI	1	4	0	0	Negative	AIDP
12	74	M	URTI	1	4	1	0	Not studied	AIDP
13	65	M	Diarrhoea	1	4	2	2[d]	Negative	Axonal GBS
14	58	M	Diarrhoea	1	4	2	2[e]	GM1	AMAN
15	58	M	URTI	3	5	1[f]	NA	Negative	AIDP

Abbreviations: F = female; GBSd = GBS disability (for definition of GBSd score, see text); M = male; NA = not applicable; URTI = upper respiratory tract infection
[a]Four further details, see Sedano et al (2019); [b]Died 5 months after onset; [c]For further details, see Berciano et al (2016); [d,e]GBSd score 18 months after onset; [f]GBSd score 8 months after onset.

was 2. All but one patient had had precedent events within 4 weeks before symptomatic onset, which were diarrhoea in 9 (60%) and upper respiratory tract infection in 5 (33%). Neither stool culture nor serology for *Campylobacter jejuni* was investigated. Upon serial evaluation up to a maximum of 24 months after onset, 7 (46.7%) cases were categorized as AIDP, 7 (46.7%) as axonal GBS, and 1 (6.6%) as unclassified GBS (Table 1 and Fig. 1).

The interval from onset to nadir was lower than 7 days in 12 (80%) cases, lower than 14 days in 2 (13%), and lower than 21 days in the remaining 1 (7%). At nadir, GBSd score was 5 (mechanically ventilated) in 5 (33%) cases, 4 in 7 (47%) cases, and 2 (20%) in the remainder. Positive anti-ganglioside reactivity occurred in 5 out of 7 patients with a final diagnosis of axonal GBS (Table 1); arbitrarily, the acronyms AMAN and AMSAN are used for cases with such reactivity, whereas axonal GBS is used when it is lacking. At admission and taking final GBS sub-typing into account, mean peak GBSd scores were 4.28 ± 0.49 for axonal GBS and 3.85 ± 1.35 for AIDP, the difference not being significant (p = 0.13). Contrariwise, at final evaluations mean GBSd score in axonal GBS, 2.43 ± 1.5, was significantly higher than that of AIDP, 0.67 ± 0.82 (p = 0.027).

There was one fatal patient (case 5 in Table 1) suffering from severe AMSAN that required continuous assisted mechanical ventilation; she died five months after the onset. Another severe AMAN patient (case 3), evolving into an AMSAN pattern, was confined to bed two years after onset (for further details of this case, see reference 20).

3.2. Electrophysiological findings

Table S2 (Supplementary material) summarizes the observed features at first electrophysiological studies performed between days 1 and 4 after onset (mean, 2.3). Altogether, motor and sensory NCS were performed in 59 and 57 nerves, respectively. Using Uncini's GBS criteria sets (Uncini et al., 2017), the most frequent changes observed in decreasing order were as follows: abnormal F waves in 28 nerves (47.5%), CMAP amplitude reduction in 27

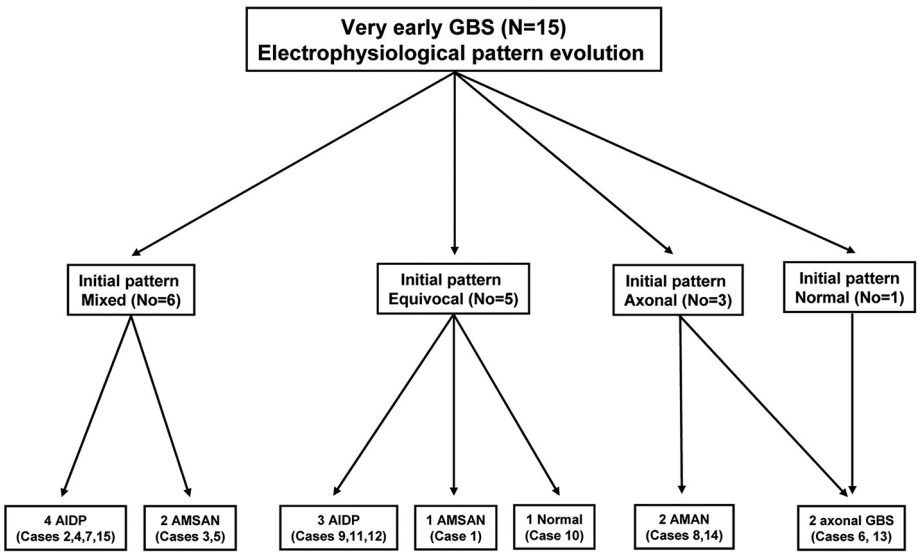

Fig. 1. Flow chart of VEGBS patient ascertainment according to initial (≤4 days after onset) and subsequent electrophysiological evaluations (dates listed in Table S2, Supplementary material). The middle panel of boxes indicates that initially accurate GBS sub-typing was only possible in 3 (20%) cases categorized as axonal pattern. Initial mixed pattern (combining criteria of both axonal failure and demyelination) evolved into either AIDP or AMSAN. Initial equivocal pattern resulted in AIDP, AMSAN or normalization. For all 3 axonal GBS patients, sub-typing did not change. The only VEGBS patient showing initial normal NCS evolved into axonal GBS. Note that after serial electrodiagnosis, disease sub-typing was not possible in 1 (6.7%) case (No. 10).

(45.7%), SNAP amplitude reduction in 18 (31.6%), reduced pCMAP/dCMAP amplitude ratio in 12 (20.3%), increase of CMAP duration in 12 (20.3%), DML prolongation in 8 (13.5%), SCV slowing in 6 (10.5%) and MCV slowing in 1 (1.7%). It is worthy of note that abnormal pCMAP/dCMAP amplitude ratios should be interpreted with caution when dCMAP is lower than 1 mV. Absent F waves occurred in 20 nerves exhibiting severe attenuation of dCMAP, whereas the remaining 8 showed delayed responses in the demyelinating range (≥120% ULN) in presence of normal or slight dCMAP amplitude reduction. In keeping with this data, the observed electrophysiological patterns (Fig. 1) were mixed, combining axonal and demyelinating features (Fig. 2), in 6 (40%) cases, equivocal in 5 (33.3%), axonal in 3 (20%), and normal in 1 (6.7%). Therefore, though initial electrophysiology showed features pointing to a peripheral nerve disorder in a high proportion of cases, early accurate sub-typing was only possible for the 3 (20%) cases showing an axonal pattern.

SNAP amplitude reduction or its absence was initially observed in 6 median nerves and 6 ulnar nerves, whereas such feature occurred in only 2 sural nerves (Table S2, Supplementary material).

As indicated in Table S2 (Supplementary material), on initial assessments there were other mild nerve conduction alterations, not conforming to Uncini's electrodiagnostic criteria sets for GBS (Uncini et al., 2017). These are MCV slowing in 13 (23%) nerves, F-wave prolongation in 13 (23%), DML increase in 11 (18.6%), SCV slowing in 11 (19.3%), dCMAP attenuation in 3 (5.3%), and SNAP amplitude reduction in 2 (3.5%). Taking together all this information into account, F-wave alteration, occurring in 70.5% out of explored nerves, was by far the commonest electrophysiological feature.

One to 4 (median 2) serial NCS were performed from the second week onwards (Table S2, Supplementary material). Final patient categorization upon serial electrophysiological evaluation is summarized in Fig. 1: i/ initial mixed pattern in six patients evolved to either AIDP (Fig. 2) or AMSAN; ii/ five patients with initial equivocal pattern resulted in AIDP, AMSAN or normalisation; iii/ all three patients with an initial axonal pattern remained under this category, here divided into either AMAN (with ganglioside reactivity) or axonal GBS (without ganglioside reactivity); and iv/ the only patient who exhibited normal initial electrodiagnosis evolved into an axonal pattern.

Initially electromyography of tibialis anterior and abductor pollicis brevis revealed a variable decrease of recruitment pattern with no spontaneous activity. On serial examination, active denervation potentials were recorded in 6 cases (Nos. 2, 3, 6–8, and 14) with primary or secondary axonal degeneration.

3.3. Ultrasonographic study

US was carried out in 14 patients between days 2 and 22 (mean, 7.0) after onset; in case 1, it was not done. The results of nerve ultrasonography are summarized in Table 2. Normative CSA values

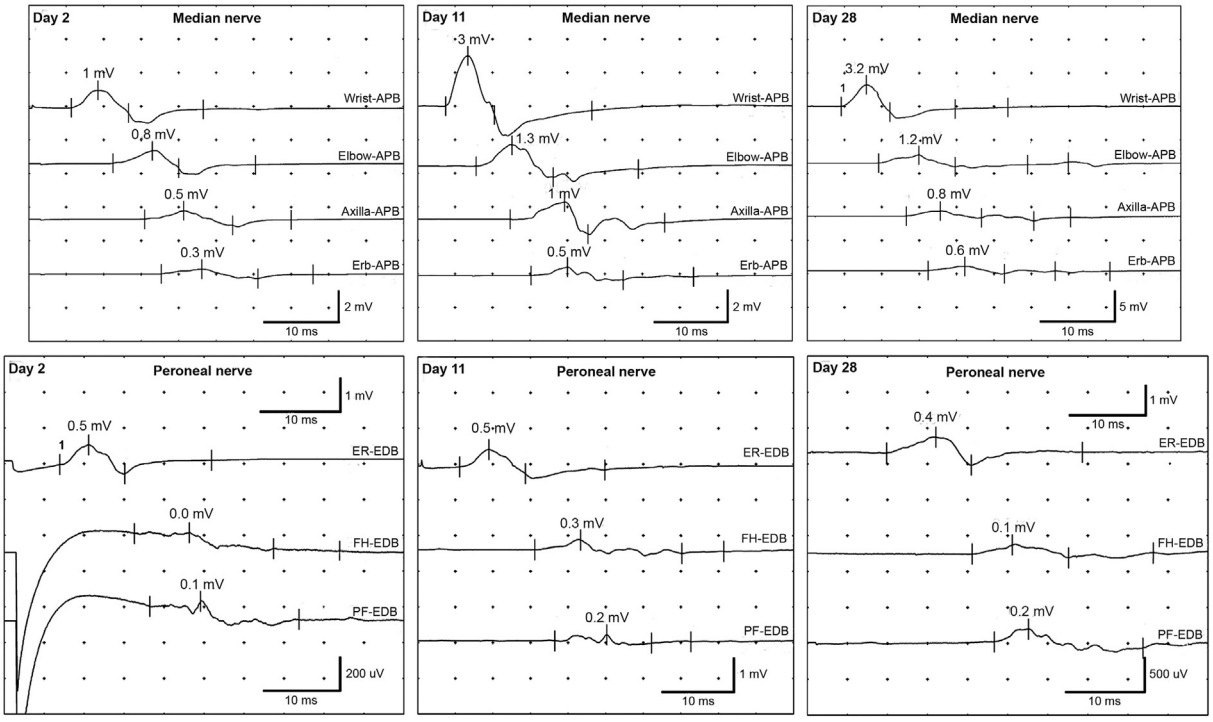

Fig. 2. Three serial NCS of median nerve and peroneal nerve in case 15, performed on days 2, 11 and 28 after onset (for clinical data see Table 1, and for initial nerve conduction values, Table S2, Supplementary material). On day 2, median nerve shows marked amplitude reduction of dCMAP (upper tracing, 1 mV; normal, ≥4 mV), pCMAP/dCMAP amplitude ratio <0.7, and pCMAP/dCMAP duration ratio >130%. There is minimal alteration of DML and MCV, dCMAP duration being preserved. On day 11, note 300% increase of dCMAP amplitude (upper tracing, 3 mV), its duration declining from 7.6 ms to 6.5 ms; consequently, these changes are indicative of RCF. pCMAP/dCMAP amplitude and duration ratios remain abnormal. MCV velocity is normal (55.4 m/s). Note CMAP temporal dispersion in three bottom tracings. On day 28, electrophysiological features are comparable to the previous study. With regard to peroneal nerve, on day 2 there is marked amplitude reduction of dCMAP that exhibits normal duration. While DML is clearly prolonged, MCV is minimally slowed (see Table S2 for values). Note the presence of CMAP desynchronization in two bottom tracings. On day 11, there are minimal variation of recordings in comparison with the previous study, excepting for an increase of dCMAP duration (8.7 ms), and decrease of MCV (30.5 m/s; 72% LLN). On day 28, the main variations are an evident increase of DML (first tracing, 9.9 ms; +180% ULN) and further decrease of MCV (28.1 m/s; 67% LLN). In short, initial mixed electrophysiological pattern has evolved into AIDP. It is worth noting that despite persistent dCMAP amplitude reduction of lower-limb nerves, clinical evolution was favourable, his GBSd score passing from 5 at admission to 1 eight months after onset. Abbreviations: APB = abductor pollicis brevis; dCMAP = distal compound motor action potential; DML = distal motor latency; EDB = extensor digitorum brevis; ER = extensor retinaculum; FH = fibular head; PF = popliteal fossa; LLN = lower limit of normal; MCV motor conduction velocity; pCMAP = proximal CMAP; ULN = upper limit of normal.

Table 2
Ultrasonography CSA values of peripheral nerve trunks in cases 2 to 15 (similar numbering as in Table 1).

Case No.	Days after onset	C5 nerve		C6 nerve		C7 nerve		Median nerve UA		Median nerve forearm		Ulnar nerve UA		Ulnar nerve forearm		Radial nerve AF		Tibial nerve PF		Tibial nerve ankle		Peroneal nerve PF		Sural nerve ankle	
		R	L	R	L	R	L	R	L	R	L	R	L	R	L	R	L	R	L	R	L	R	L	R	L
2	5	6	6	7	11	8	13	9	7	7	7	6	5	6	5	4	5	24	17	14	15	18	21	2	1
3	3	6	5	11	13	6 BB	NA	7	16	7	10	7	10	5	NA	8	8	25	37	15	17	12	11	2	2
4	6	6 BB	3	10 BB	10	10 BB	8	5	14	5	6	4	7	5	5	3	6	15	19	12	15	13	15	3	3
5	22	6 BB	6 BB	10 BB	15 BB	16 BB	21 BB	9	9	11	7	6	6	8	6	NA	NA	15	14	12	12	7	8	NA	NA
6	3	9 BB	9 BB	14 BB	12	27	17	9	12	6	7	10	7	5	5	4	5	18	21	14	11	6	9	2	3
7	10	8 BB	11 BB	28 BB	13 BB	22 BB	19 BB	11	9	8	7	8	10	4	9	4	4	19	23	16	19	7	8	NA	NA
8	4	20	12	25 BB	20 BB	29 BB	22 BB	12	12	6	7	11	7	7	7	6	3	46	45	17	19	22	8	2	5
9	2	8	8	8	9	6	8	7	6	7	5	5	7	4	4	3	3	15	18	10	9	12	14	3	3
10	8	13 BB	12 BB	18 BB	16 BB	12	16	17	19	8	7	10	10	8	6	7	7	33	24	16	12	13	9	4	2
11	10	12 BB	11 BB	30 BB	26 BB	18 BB	23 BB	14	10	6	7	7	8	6	5	5	6	33	34	10	21	9	6	2	3
12	6	14 BB	8 BB	20 BB	18 BB	25 BBV	22 BB	12	9	8	5	12	13	11	6	5	6	NA	NA	21	34	NA	NA	NA	NA
13	5	13 BB	11	35 BB	15	43 BB	14	14	19	9	9	11	13	9	7	9	6	14	33	36	25	12	10	3	4
14	12	14	16 BB	19 BB	18 BB	44 BB	26 BB	15	12	8	8	11	7	5	5	5	NA	16	28	13	15	10	11	3	3
15	2	7	5	16	19	15 BB	18 BB	12	17	7	6	9	5	6	6	6	12	23	21	12	12	6	8	NA	NA
Mean (SD)	7.0 (5.3)	10.1[a] (4.3)	8.8[b] (3.6)	17.9[c] (8.8)	15.4[d] (4.6)	20.1[e] (12.4)	17.5[a] (5.6)	10.9[f] (3.4)	12.2[g] (4.2)	7.4 (1.5)	7.0 (1.4)	8.4[f] (2.6)	8.2[h] (2.6)	6.4 (2.0)	5.3 (1.3)	5.3 (1.8)	5.9 (2.4)	22.8 (9.6)	25.7 (9.1)	15.6 (6.6)	16.9 (6.6)	11.3 (4.7)	10.6 (4.0)	2.6 (0.7)	2.9 (1.1)

Abbreviations: AF = antecubital fossa; BB = blurred boundaries (ventral rami of C5-C7 nerves); CSA = cross sectional area; NA = not available; PF = popliteal fossa; R = right; L = left; UA = upper arm.
Underlined values are those over X + 2SD of normative values reported in the literature (Cartwright et al., 2008; Kerasnoudis et al., 2014; Gallardo et al., 2015a)
Statistical significance of enlarged mean CSA values of C5-C7 nerves compared with those reported by Gallardo et al., (2015a): (a) $p < 0.004$; (b) $p < 0.01$; (c) $p < 0.002$; (d) $p < 0.0004$; (e) $p < 0.03$.
Statistical significance of enlarged mean CSA values of proximal median and ulnar nerves compared with those reported by Kerasnoudis et al. (2014): (f) $p < 0.02$; (g) $p < 0.006$; (h) $p < 0.04$.

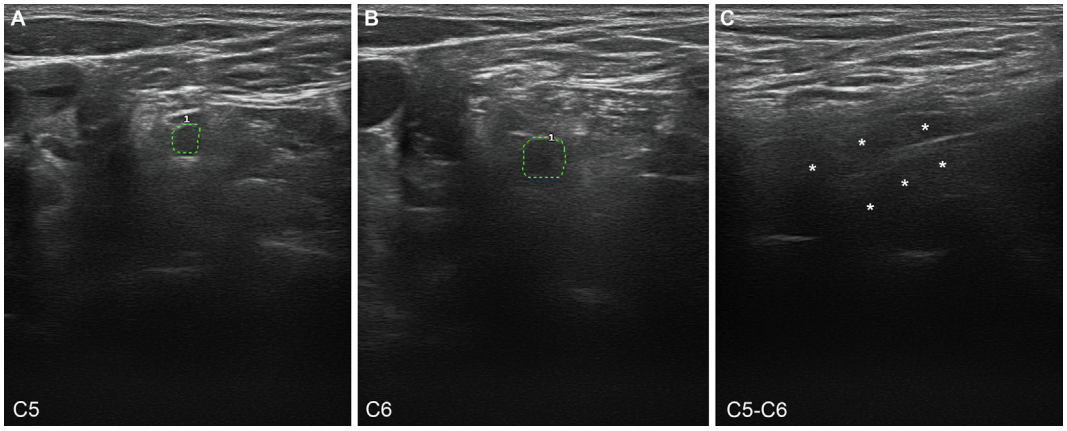

Fig. 3. US of the ventral rami of the left fifth and sixth cervical nerves of case 12 with initial equivocal electrophysiological pattern evolving into AIDP (see Table 1 and Fig. 1); sonograms were obtained on day 6 after onset. (A and B) Short-axis sonograms showing enlarged CSAs of both cervical nerves (dotted green tracings; for values see Table 2); note that perineurial hyperechoic rims are not identified and that the edge between the nerve and the surrounding fat is not clear. (C) Sagittal sonograms showing blurred of boundaries of both nerves (asterisks). (For interpretation of the references to colour in this figure legend, the reader is referred to the web version of this article.)

of median, ulnar, radial, peroneal, tibial, sural and ventral rami of C5–C7 nerves were taken from those reported in the literature (Cartwright et al., 2008; Kerasnoudis et al., 2014; Gallardo et al., 2015a). Figs. 3 and 4 illustrate the main sonographic finding that relied on ventral rami of C5–C7 nerves, which consisted of a variable combination of symmetric or asymmetric blurred boundaries and significant increase of CSA (Table 2). Loss of the physiologic hyperechoic perineurial rim was observed between 50% and 71.4% of individual scanned cervical nerves; CSA enlargement ranged from 35.7% to 57.1%. Although, most enlarged spinal nerves also exhibited blurred boundaries, there were examples showing one of the two changes in isolation. C5–C7 sonographic findings were similar in patients eventually categorized as AMAN/AMSAN or AIDP. It is worth noting that just 2 cases (14.3%) showed entirely normal C5-C7 nerve sonograms.

In more distant nerve trunks sonographic changes were scanty and consisted of increased CSA, which at most involved 4 (28.6%) left median nerves and 4 (28.6%) right ulnar nerves at upper-arm level; increase of mean CSA was only significant for median and ulnar nerves at upper-arm level (Table 2). At forearm level, enlarged CSA was just observed in 2 (14.3%) right ulnar nerves and 1 (7.1%) right median nerve; radial nerve was always normal. In lower-limb nerves, enlarged CSA was observed at most in 2 (14.3%) left tibial nerves at ankle; sural nerve was always preserved.

4. Discussion

In the 8-year period of the current study, 15 VEGBS adult patients were identified, upon whom serial electrophysiological studies were available, the initial ones having always been performed within the first four days of the clinical course. For the first time, we used the optimized electrodiagnostic criteria recently reported by Uncini and colleagues for subtype GBS classification (Uncini et al., 2017). Furthermore and as soon as practicable, in 14 patients we performed nerve US in order to correlate early electrophysiological features and topographic US nerve changes. The series included 14 patients with classic GBS, and one patient with paraparetic GBS (Wakerley et al., 2014; Berciano et al., 2016). We have to admit that selection of VEGBS patients inevitably implies that one is dealing with severe disease forms admitted promptly to the hospital; in fact, 80% of cases showed severe peak GBSd scores, 4 or 5, as opposed to 51.3% observed in our recent, unbiased GBS survey (Sedano et al., 2019).

4.1. Electrophysiological features

In our series, initial NCS indicate that accurate VEGBS subtyping was just possible for the 3 (20%) patients showing an axonal pattern; intriguingly, this subtype did not change on serial evaluation. In the remaining 12 (80%) cases, initial NCS revealed mixed pattern (combining the criteria of both axonal dysfunction and demyelination) in 6, equivocal pattern in 5 (not fulfilling any of the AIDP or axonal GBS criteria) and normal pattern in 1. Upon serial electrophysiological evaluation, GBS subtypes were set down as follows: 7 AIDP, 7 axonal GBS and 1 unclassified (see Fig. 1)

There are just four previous clinical-electrophysiological studies in VEGBS (Gordon and Wilbourn, 2001; Albertí et al., 2011; Chanson and Echaniz-Laguna, 2014; Jin et al., 2018). Gordon and Wilbourn (2001) carried out early electrodiagnostic studies in 31 cases GBS patients, in 8 of them within ≤4 days. Although absent H reflex was observed in 7 (88%) cases, they stated that "Electrodiagnostic studies performed before the fifth day were likely to be non-diagnostic". Albertí et al. (2011) studied 18 VEGBS adult patients with follow-up at 3 months being available in 14 of them. While 15 (83%) cases showed abnormal motor conduction parameters, only 5 (27%) fulfilled their criteria for AIDP and 1 (6%) for the axonal variant of GBS, namely 12 (67%) cases eventually were classified as equivocal. In the comprehensive early AIDP series reported by Chanson and Echaniz-Laguna (2014), there was a subgroup of 21 cases examined ≤4 days, whose electrodiagnostic reliability was extremely variable, ranging between 19% using Cornblath criteria (Cornblath, 1990) and 65% applying their own proposed criteria. In a recent study, Jin et al. (2018) reported electrophysiological features in 51 GBS patients classified into 3 subgroups according to the intervals of symptom onset and NCS, namely 1–4 days (11 cases), 5–10 days (20 cases) and >10 days (20 cases). One case of the very early subgroup showed normal neurophysiological findings, while the remaining 10 patients displayed abnormal features; contrary to what might be expected from our results, comparison of inter-subgroup percentages of electrophysiological changes did not show significant differences.

Chanson and Echaniz-Laguna (2014) have tabulated in detail so far reported VEGBS electrophysiological features (see their Table 1). Although we adhered to GBS optimized electrodiagnosis (Uncini et al., 2017), there is, to some degree, certain parallelism between results in previous VEGBS series and those reported here, namely: i/ abnormal F waves, 55–75% (here, 47.5%); ii/ dCMAP attenuation, 37–57% (55%); iii/ SNAP attenuation, 25–44% (31.6%); iv/ DML prolongation in the demyelinating range, 33–38% (13.5%); and v/ MCV

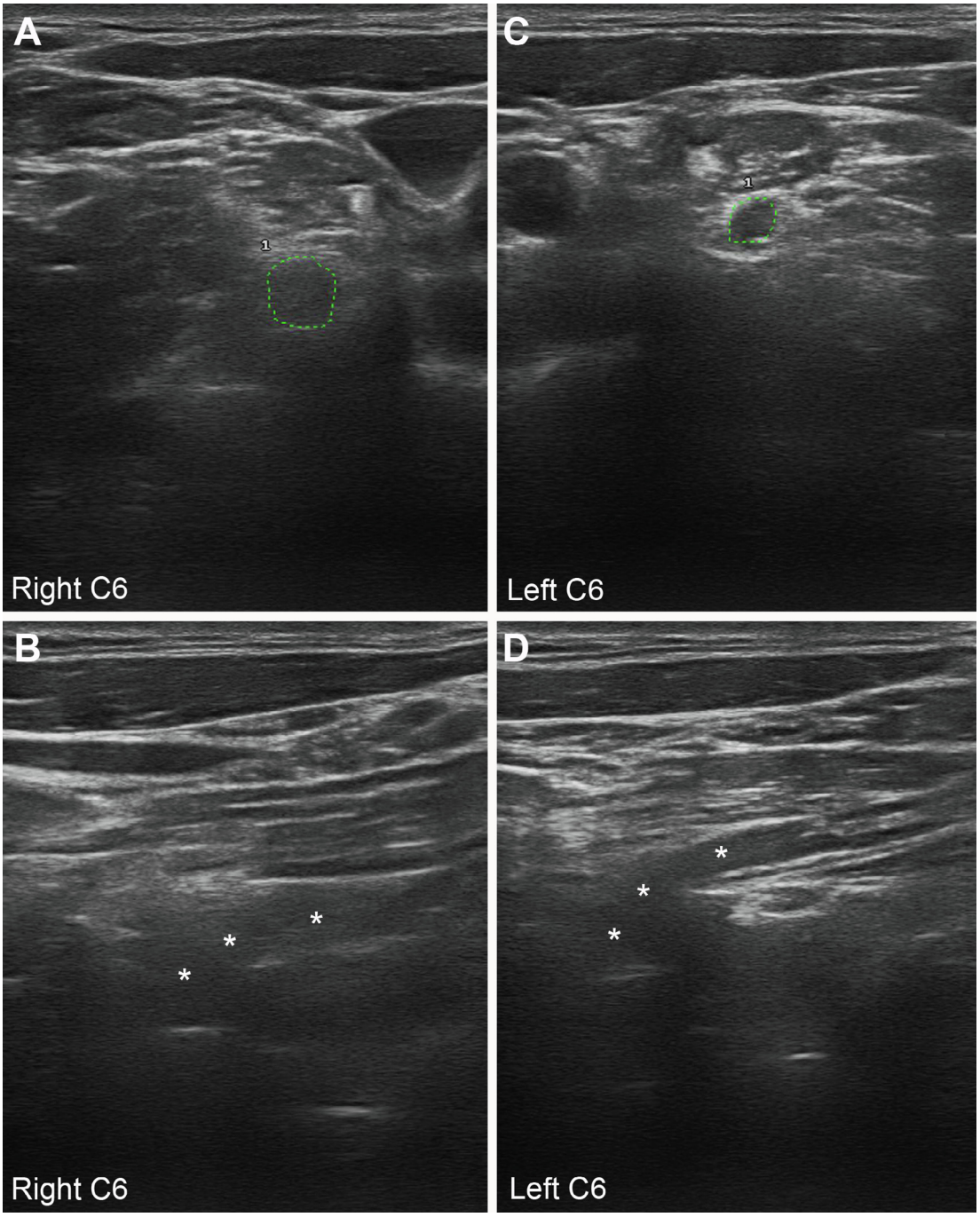

Fig. 4. US of the ventral rami of the sixth cervical nerves of case 13 with a final diagnosis of axonal GBS (see Table 1 and Fig. 1); sonograms were obtained on day 5 after onset. (A) Short-axis sonogram showing marked CSA enlargement of the right C6 nerve (dotted green tracing; for values, see Table 2), its perineurial rim not being identified. (B) In this sagittal sonogram the right C6 nerve (asterisks), note also disappearance of perineurial rim.(C) Short-axis sonogram of the left C6 nerve showing normal CSA (dotted green tracing; for values, see Table 2) with preservation of the perineurial hyperechoic rim. (D) Sagittal sonogram of the left C6 nerve (asterisks) illustrating quite well preservation of its perineurial hyperechoic rim. (For interpretation of the references to colour in this figure legend, the reader is referred to the web version of this article.)

slowing >1 nerve 12–66% (1.7%). It is worth noting that taking together optimized abnormal electrophysiological features and mild nerve conduction changes, not conforming to Uncini's GBS electrodiagnostic criteria (Uncini et al., 2017), alteration of F waves was the most frequent finding involving here 70.5% of examined motor nerves.

4.2. Ultrasound features

The current nerve US study corroborates that main lesions rely on ventral rami of C5–C7 nerves occurring equally in patients finally categorized as axonal GBS or AIDP (Gallardo et al., 2015a). Spinal nerves are usually monofascicular with epi-perineural covering, which accounts for their sonographic appearance consisting of hypoechoic oval structure surrounded by hyperechoic perineurial rim (Haun et al., 2010). Autopsy studies in early AIDP have demonstrated that initial lesion is inflammatory oedema predominating in spinal roots and ventral rami of spinal nerves (Haymaker and Kernohan, 1949; Krücke, 1955; Berciano et al., 2017). Intriguingly, such topography of lesions concurs with that originally found in AMAN, literally reported as follows (McKhann et al., 1993): "The most proximal site of fibre degeneration was in the

proximal or mid-ventral roots; the proportion of degenerating fibres increased distally toward the ventral root exit from the dura. At this level, up to 80% of motor fibres were degenerating". According to such pathological notions, our main sonographic findings include a variable combination of significant CSA enlargement of C5–C7 nerves and blurred boundaries. Furthermore, the observed high prevalence of early F-wave alterations in our and other series also point to pathological changes in proximal nerve trunks (Berciano et al., 2017). Experimentally, blood-nerve interface is less efficient in several important structures in the peripheral nervous system, including from the spinal cord to the root-nerve junction (spinal nerve), dorsal root ganglia and neuromuscular junctions (Olsson, 1968; Kanda, 2013); hence these sites are believed to be especially vulnerable to inflammatory neuropathies. In addition, the pathogenic relevance of proximal nerve trunk lesions in AIDP and AMAN has been demonstrated by means of lumbar root stimulation (Kurt Incesu et al., 2013) and triple stimulation technique (Sevy et al., 2018), respectively.

In more peripheral nerve trunks, our US study showed that significant CSA enlargement occurs only in median and ulnar nerves at upper-arm level. In a previous VEGBS sonographic investigation, significant enlargement was found in all measured nerves, except the sural nerve (Grimm et al., 2016). The obvious discrepancy calls for new US studies.

4.3. Pathophysiological considerations

Experimental autoimmune neuritis (EAN) has provided some important information regarding the pathogenic mechanisms of GBS (Soliven, 2012). We will focus on some of them to decipher certain electrophysiological findings described here. In EAN mediated by P2-reactive T-cell lines in Lewis rats, flaccid tail and weakness of the hindlimbs start 3.5–4 days post-inoculation (pi), whereas the first evidence of pathologic change, consisting of severe epi-perineurial and endoneurial inflammatory oedema in the sciatic nerve, comes out 4 days pi, obvious demyelination and axonal degeneration appearing between days 7 and 9 (Izumo et al., 1985). In L5 root, at peak disease (day 6) the mean number of demyelinated axons is 79/mm^2 (0.7% of the total number), and of degenerating axons is 121/mm^2 (1.0% of the total) (Hadden et al., 2002); certainly, such low percentage of nerve fibre degeneration does not seem sufficient to explain maximal neurologic deficit (complete limb paralysis). In nerves possessing epi-perineurium, axonal damage appears at the height of the inflammatory process (day 7 pi), when oedema and increase of endoneurial pressure are maximal, which are believe to stretch the perineurium and constrict the transperineurial microcirculation, compromising nerve blood flow and producing the potential for ischemic nerve injury (Powell et al., 1991; Powell and Myers, 1996). Such mechanism has been illustrated in a clinico-patological study of a severe AIDP patient (Berciano et al., 2000).

The notion that nerve inflammatory oedema might be pathogenic in VEGBS, when neither full-blown demyelination nor wallerian-like degeneration has entered into the scene, helps clarify some of our initial electrophysiological findings, namely:

- Mixed pattern observed in 40% of our patients, which evolved into either AIDP or AMSAN, is probably accounted for by ischemic injury of distal peripheral nerve trunks causing dysfunction of conducting myelinated fibres, axons, or both. Given that such nerve segments are not amenable to sonography and histological studies of terminal and pre-terminal nerve segments are lacking, serial proximal-to-distal nerve trunk histological studies in fatal VEGBS seem to be a pressing need.
- In axonal VEGBS with normal electrophysiology, the presence of sonographic changes in ventral rami of C5-C7 nerves point to a proximal nerve conduction block as the mechanism of paralysis.
- It is a well-established fact that in AMAN/AMSAN anti-ganglioside antibodies bind to axolemma causing conduction failure and eventually axonal degeneration (Rajabally et al., 2015; Uncini et al., 2017; Uncini and Kuwabara, 2018). In our axonal cases, US regularly showed changes in ventral rami of C5-C7 nerves. Therefore, we propose that in very early AMAN there may be a dual mechanism of muscle weakness: i/ ganglioside-mediated distal motor conduction block, not amenable to US visualization; and ii/ conduction block at ventral rami of spinal nerves induced by inflammatory oedema.
- Characteristic of AMAN/AMSAN is dCMAP attenuation with normal duration. Here we report an AMSAN patient with widespread amplitude reduction of dCMAPs accompanied by reversible increase of their duration (see Table S2; Supplementary material). This phenomenon could be associated with early but regressive inflammatory events of pre-terminal nerve trunks causing ischemic dysfunction of motor conduction fibres.
- RCF is one of the hallmarks of AMAN. Here we describe this phenomenon in an AIDP patient with no ganglioside reactivity (see Fig. 2B). Again, its pathophysiology could be correlated with early inflammatory oedema of distal nerve trunks.

5. Limitations

The present study has limitations including the retrospective nature, the reduced number of patients collected from a single hospital, the absence of scheduled dates for serial NCS, and no concomitance between initial NCS and nerve sonographic study. For better pathogenic understanding we need large and prospective electrophysiological and ultrasonographic studies in very early stages of the disease, which should be done on a multinational, multicenter basis.

6. Conclusion

In VEGBS serial electrophysiological evaluation is necessary for accurate subtype classification. Nerve ultrasonography helps delineate the topography of changes in early stages of the disease.

Acknowledgement

This paper was supported by IDIVAL (ID APG/11) and CIBERNED. The authors are most grateful to Mrs Marta de la Fuente for secretarial assistance.

Conflicts of interest

None of the authors have potential conflicts of interest to be disclosed.

Appendix A. Supplementary data

Supplementary data to this article can be found online at https://doi.org/10.1016/j.cnp.2019.11.003.

References

Albertí, M.A., Alentorn, A., Martínez-Yelamos, S., Martínez-Matos, J.A., Povedano, M., Montero, J., et al., 2011. Very early electrodiagnostic findings in Guillain-Barré syndrome. J. Peripher. Nerv. Syst. 16, 136–142.

Asbury, A.K., Cornblath, D.R., 1990. Assessment of current diagnostic criteria for Guillain-Barré syndrome. Ann. Neurol. (27 Suppl), S21–S24
Berciano, J., García, A., Figols, J., Muñoz, R., Berciano, M.T., Lafarga, M., 2000. Perineurium contributes to axonal damage in acute inflammatory demyelinating polyneuropathy. Neurology 55, 552–559.
Berciano, J., Gallardo, E., Orizaola, P., de Lucas, E.M., García, A., Pelayo-Negro, A.L., et al., 2016. Early axonal Guillain-Barré syndrome with normal peripheral conduction: imaging evidence for changes in proximal nerve segments. J. Neurol. Neurosurg. Psychiatry 87, 563–565.
Berciano, J., Sedano, M.J., Pelayo-Negro, A.L., García, A., Orizaola, P., Gallardo, E., et al., 2017. Proximal nerve lesions in early Guillain-Barré syndrome: implications for pathogenesis and disease classification. J. Neurol. 264, 221–236.
Cartwright, M.S., Passmore, L.V., Yoon, J.S., Brown, M.E., Caress, J.B., Walker, F.O., 2008. Cross-sectional area reference values for nerve ultrasonography. Muscle Nerve 37, 566–571.
Chanson, J.B., Echaniz-Laguna, A., 2014. Early electrodiagnostic abnormalities in acute inflammatory demyelinating polyneuropathy: a retrospective study of 58 patients. Clin. Neurophysiol. 125, 1900–1905.
Clouston, P.D., Kiers, L., Zuniga, G., Cros, D., 1994. Quantitative analysis of the compound muscle action potential in early acute inflammatory demyelinating polyneuropathy. Electroencephalogr. Clin. Neurophysiol. 93, 245–254.
Cornblath, D.R., 1990. Electrophysiology in Guillain-Barré syndrome. Ann. Neurol. 27 (Suppl), S17–S20.
Doets, A.Y., Verboon, C., van den Berg, B., Harbo, T., Cornblath, D.R., Willison, H.J., et al., 2019. IGOS Consortium. Regional variation of Guillain-Barré syndrome. Brain 141, 2866–2877.
Gallardo, E., Sedano, M.J., Orizaola, P., Sánchez-Juan, P., González-Suárez, A., García, A., et al., 2015a. Spinal nerve involvement in early Guillain-Barré syndrome: a clinico-electrophysiological, ultrasonographic and pathological study. Clin. Neurophysiol. 126, 810–819.
Gallardo, E., Noto, Y., Simon, N.G., 2015b. Ultrasound in the diagnosis of peripheral neuropathy: structure meets function in the neuromuscular clinic. J. Neurol. Neurosurg. Psychiatry 86, 1066–1074.
Gordon, P.H., Wilbourn, A.J., 2001. Early electrodiagnostic findings in Guillain-Barré syndrome. Arch. Neurol. 58, 913–917.
Griffin, J.W., Li, C.Y., Ho, T.W., Tian, M., Gao, C.Y., Xue, P., et al., 1996. Pathology of the motor-sensory axonal Guillain-Barré syndrome. Ann. Neurol. 39, 17–28.
Grimm, A., Décard, B.F., Axer, H., 2014. Ultrasonography of the peripheral nervous system in the early stage of Guillain-Barré syndrome. J. Peripher. Nerv. Syst. 19, 234–241.
Grimm, A., Décard, B.F., Schramm, A., Pröbstel, A.K., Rasenack, M., Axer, H., et al., 2016. Ultrasound and electrophysiologic findings in patients with Guillain-Barré syndrome at disease onset and over a period of six months. Clin. Neurophysiol. 127, 1657–1663.
Hadden, R.D., Cornblath, D.R., Hughes, R.A., Zielasek, J., Hartung, H.P., Toyka, K.V., et al., 1998. Electrophysiological classification of Guillain-Barré syndrome: clinical associations and outcome. Plasma exchange/Sandoglobulin Guillain-Barré Syndrome Trial, Group. Ann. Neurol. 44, 780–788.
Hadden, R.D., Gregson, N.A., Gold, R., Smith, K.J., Hughes, R.A., 2002. Accumulation of immunoglobulin across the 'blood-nerve barrier' in spinal roots in adoptive transfer experimental autoimmune neuritis. Neuropathol. Appl. Neurobiol. 28, 489–497.
Haun, D.W., Cho, J.C., Kettner, N.W., 2010. Normative cross-sectional area of the C5–C8 nerve roots using ultrasonography. Ultrasound Med. Biol. 36, 1422–1430.
Haymaker, W.E., Kernohan, J.W., 1949. The Landry-Guillain-Barré syndrome; a clinicopathologic report of 50 fatal cases and a critique of the literature. Medicine (Baltimore) 28, 59–141.
Izumo, S., Linington, C., Wekerle, H., Meyermann, R., 1985. Morphologic study on experimental allergic neuritis mediated by T cell line specific for bovine P2 protein in Lewis rats. Lab. Invest. 53, 209–218.
Jin, J., Hu, F., Qin, X., Liu, X., Li, M., Dang, Y., et al., 2018. Very early neurophysiological study in Guillain-Barre syndrome. Eur. Neurol. 80, 100–105.
Kanda, T., 2013. Biology of the blood-nerve barrier and its alteration in immune mediated neuropathies. J. Neurol. Neurosurg. Psychiatry 84, 208–212.
Kerasnoudis, A., Pitarokoili, K., Behrendt, V., Gold, R., Yoon, M.S., 2014. Nerve ultrasound score in distinguishing chronic from acute inflammatory demyelinating polyneuropathy. Clin. Neurophysiol. 125, 635–641.
Krücke, W., 1955. Die primär-entzündliche Polyneuritis unbekannter Ursache. In: Lubarsch, O. (Ed.), Handbuch der speziallen pathologischen Anatomie und Histologie, Vol XIII/5, Erkrankungen des peripheren und des vegetativen Nerven. Springer-Verlag, Berlin.
Kurt Incesu, T., Secil, Y., Tokucoglu, F., Gurgor, N., Özdemirkiran, T., Akhan, G., et al., 2013. Diagnostic value of lumbar root stimulation at the early stage of Guillain-Barré syndrome. Clin. Neurophysiol. 124, 197–203.
McKhann, G.M., Cornblath, D.R., Griffin, J.W., Ho, T.W., Li, C.Y., Jiang, Z., et al., 1993. Acute motor axonal neuropathy: a frequent cause of acute flaccid paralysis in China. Ann. Neurol. 33, 333–342.
Olsson, Y., 1968. Topographical differences in the vascular permeability of the peripheral nervous system. Acta Neuropathol. 10, 26–33.
Powell, H.C., Myers, R.R., Mizisin, A.P., Olee, T., Brostoff, S.W., 1991. Response of the axon and barrier endothelium to experimental allergic neuritis induced by autoreactive T cell lines. Acta Neuropathol. 82, 364–377.
Powell, H.C., Myers, R.R., 1996. The axon in Guillain-Barré syndrome: immune target or innocent bystander? Ann. Neurol. 39, 4–5.
Rajabally, Y.A., Durand, M.C., Mitchell, J., Orlikowski, D., Nicolas, G., 2015. Electrophysiological diagnosis of Guillain-Barré syndrome subtype: could a single study suffice? J. Neurol. Neurosurg. Psychiatry 86, 115–119.
Sedano, M.J., Calleja, J., Canga, E., Berciano, J., 1994. Guillain-Barré syndrome in Cantabria, Spain. An epidemiological and clinical study. Acta Neurol. Scand. 89, 287–292.
Sedano, M.J., Orizaola, P., Gallardo, E., García, A., Pelayo-Negro, A.L., Sánchez-Juan, P., et al., 2019. A unicenter, prospective study of Guillain-Barré syndrome in Spain. Acta Neurol. Scand. 139, 546–554.
Sevy, A., Grapperon, A.M., Salort Campana, E., Delmont, E., Attarian, S., 2018. Detection of proximal conduction blocks using a triple stimulation technique improves the early diagnosis of Guillain-Barré syndrome. Clin. Neurophysiol. 129, 127–132.
Soliven, B., 2012. Autoimmune neuropathies: insights from animal models. J. Peripher. Nerv. Syst. 17 (Suppl 2), 28–33.
Uncini, A., Kuwabara, S., 2018. The electrodiagnosis of Guillain-Barré syndrome subtypes: where do we stand? Clin. Neurophysiol. 129, 2586–2593.
Uncini, A., Ippoliti, L., Shahrizaila, N., Sekiguchi, Y., 2017. Kuwabara. Optimizing the electrodiagnostic accuracy in Guillain-Barré syndrome subtypes: criteria sets and sparse linear discriminant analysis. Clin. Neurophysiol. 128, 1176–1183.
van den Berg, B., Walgaard, C., Drenthen, J., Fokke, C., Jacobs, B.C., van Doorn, P.A., 2014. Guillain-Barré syndrome: pathogenesis, diagnosis, treatment and prognosis. Nat. Rev. Neurol. 10, 469–482.
Vucic, S., Cairns, K.D., Black, K.R., Chong, P.S., Cros, D., 2004. Neurophysiologic findings in early acute inflammatory demyelinating polyradiculoneuropathy. Clin. Neurophysiol. 115, 2329–2335.
Wakerley, B.R., Uncini, A., Yuki, N., 2014. GBS Classification Group. Guillain-Barré and Miller Fisher syndromes-new diagnostic classification. Nat. Rev. Neurol. 10, 537–544.
Winer, J.B., Hughes, R.A., Osmond, C., 1988. A prospective study of acute idiopathic neuropathy. I. Clinical features and their prognostic value. J. Neurol. Neurosurg. Psychiatry 51, 605–612.